Rapidity Dependence of Charged Antiparticle-to-Particle Ratios in Au+Au Collisions at $\sqrt{s_{NN}} = 200$ GeV

I. G. Bearden[7], D. Beavis[1], C. Besliu[10], Y. Blyakhman[6], B. Budick[6], H. Bøggild[7], C. Chasman[1], C. H. Christensen[7], P. Christiansen[7], J. Cibor[3], R. Debbe[1], E. Enger[12], J. J. Gaardhøje[7], M. Germinario[7], K. Hagel[8], O. Hansen[7], A. Holm[7], A. K. Holme[12], H. Ito[11], E. Jakobsen[7], A. Jipa[10], F. Jundt[2], J. I. Jørdre[9], C. E. Jørgensen[7], R. Karabowicz[4], T. Keutgen[8], E. J. Kim[1], T. Kozik[4], T. M. Larsen[12], J. H. Lee[1], Y. K. Lee[5], G. Løvhøiden[12], Z. Majka[4], A. Makeev[8], B. McBreen[1], M. Mikelsen[12], M. Murray[8], J. Natowitz[8], B. S. Nielsen[7], J. Norris[11], K. Olchanski[1], J. Olness[1], D. Ouerdane[7], R. Płaneta[4], F. Rami[2], C. Ristea[10], D. Röhrich[9], B. H. Samset[12], D. Sandberg[7], S. J. Sanders[11], R. A. Scheetz[1], P. Staszel[7], T. S. Tveter[12], F. Videbæk[1], R. Wada[8], A. Wieloch[4], Z. Yin[9], I. S. Zgura[10]
The BRAHMS Collaboration

[1] Brookhaven National Laboratory, Upton, New York 11973, USA
[2] Institut de Recherches Subatomiques and Université Louis Pasteur, Strasbourg, France
[3] Institute of Nuclear Physics, Krakow, Poland
[4] Smoluchkowski Inst. of Physics, Jagiellonian University, Krakow, Poland
[5] Johns Hopkins University, Baltimore 21218, USA
[6] New York University, New York 10003, USA
[7] Niels Bohr Institute, Blegdamsvej 17, University of Copenhagen, Copenhagen 2100, Denmark
[8] Texas A&M University, College Station, Texas, 17843, USA
[9] University of Bergen, Department of Physics, Bergen, Norway
[10] University of Bucharest, Romania
[11] University of Kansas, Lawerence, Kansas 66049, USA
[12] University of Oslo, Department of Physics, Oslo, Norway

(Dated: Version: RatioDraft4.0.tex, July 12, 2002)

We present ratios of the numbers of charged antiparticles to particles (pions, kaons and protons) in Au + Au collisions at $\sqrt{s_{NN}} = 200$ GeV as a function of rapidity in the range y=0-3. While the particle ratios at midrapidity are approaching unity, the K^-/K^+ and $\bar{p}/p$ ratios decrease significantly at forward rapidities. An interpretation of the results within the statistical model indicates a reduction of the baryon chemical potential from $\mu_B \approx 130$MeV at y=3 to $\mu_B \approx 25$MeV at y=0.

PACS numbers: 25.75 Dw.

Ratios of yields of particles to antiparticles and, in particular the rapidity dependence of such ratios, are significant indicators of the dynamics of high energy nucleus-nucleus collisions [1, 2]. At the energy of $\sqrt{s_{NN}}$=200 GeV considerable transparency is expected for Au+Au collisions, even for central events. This should lead to a flat multiplicity density as function of rapidity (y) near midrapidity, and $\bar{p}/p$ and K^-/K^+ particle yield ratios with values near unity. Away from midrapidity the net baryon content originating from the initial nuclei is significant and production mechanisms other than particle-antiparticle pair production play a substantial role. Therefore $\bar{p}/p$ and K^-/K^+ ratios will decrease with increasing rapidity $|y|$. Measurements of $\bar{p}/p$ ratios at 130 GeV [3–6] and of pseudo-rapidity distributions of charged particles at 130 GeV [7] and 200 GeV [8, 9] point to the development described above, reminiscent of the Bjorken picture [10].

In the present Letter measurements of ratios $\pi^-/\pi^+, K^-/K^+$ and $\bar{p}/p$ as a function of rapidity, transverse momentum (p_T) and collision centrality (top 20%) are presented for Au+Au collisions at $\sqrt{s_{NN}} = 200$ GeV. We measure $\langle d^2n/dp_T dy\rangle \Delta p_T \Delta y$, where the averaging is over phase space, $\Delta p_T \Delta y$. The ratios are for the normalized numbers of detected particles, including corrections as described below.

At midrapidity, the measured antiparticle to particle ratios are approaching unity, i.e. they vary between 0.75 ± 0.04 ($\bar{p}/p$), 0.95 ± 0.05 (K^-/K^+) to 1.01 ± 0.04 (π^-/π^+). These values exceed the corresponding ratios measured for Pb+Pb reactions at ($\sqrt{s_{NN}} = 17$ GeV) by factors of about 1.8 for the kaons and by about 10 for the protons. Recent PHOBOS measurements [11] are consistent with the y=0 measurements presented here.

While the pion ratios are consistent with unity over the entire rapidity range covered, the ratios of the strange mesons and of the baryons drop to $K^-/K^+ = 0.67 \pm 0.06$ and $\bar{p}/p = 0.23 \pm 0.03$ at $y \approx 3$. This behavior supports the idea of the formation of a nearly net-baryon free zone at midrapidity in the collisions

where particle production is dominated by pair creation, either at the quark level or at the hadron level. However, towards larger rapidities, the ratios become increasingly influenced by the baryon content of the original nuclei. The present work indicates an increase, at $y = 0$, of the ratios relative to $\sqrt{s_{NN}} = 130$ GeV Au+Au collisions of about 5% for kaons and of about 17% for protons [3–6].

The data were obtained with the BRAHMS detector, which consists of two independent small-aperture magnetic spectrometers that can rotate in the horizontal plane about the nominal interaction point (IP), covering the rapidity range $-0.1 < y < 4$ for pions and $-0.1 < y < 3.4$ for protons. Details may be found in Ref. [12]. The MidRapidity Spectrometer (MRS) consists of two time projection chambers (TPC) and a magnet, for determining particle momenta. This assembly is followed by a segmented scintillator time–of–flight wall (TOFW), with time resolution $\sigma_t \approx 75$ps, for particle velocity measurements. Requiring a $\pm 2\sigma_t$ cut around the expected flighttime, π-K separation is achieved up to a momentum of 2.3 GeV/c and K-p separation up to 3.9 GeV/c. The Front Forward Spectrometer (FFS) consists, in order, of a dipole magnet, a TPC, a second dipole magnet, a second TPC, a time–of–flight wall (TOF1) and a threshold gas-Cherenkov detector (C1). At small polar angles (from 2.3° to 15°), where the mean momentum of particles is large, a back section (BFS) with two dipole magnets, three drift chambers, a time of flight wall (TOF2) and a ring imaging Cherenkov detector (RICH) is also used. TOF1 (at 8.6 m) and TOF2 (at 18 m) allow for K-p separation up to p=5.5 and 8 GeV/c, respectively. C1 identifies pions in the range from $p = 3$ to 9 GeV/c and the RICH allows π-K separation up to $p = 25$ GeV/c and K-p separation from p=10 to p=35 GeV/c.

The reaction centrality was determined using a plastic scintillator tile array surrounding the intersection region [7, 8, 12]. Beam-Beam Counters (BBCs) consisting of two arrays of Cherenkov radiators positioned ± 2.15 m from the IP were used to measure charged hadrons in the pseudo-rapidity range $3.0 < |\eta| < 3.8$. For the most 25% central collisions, the BBCs allow collision vertex determination with resolution $\sigma_z \approx 0.65$ cm and supply the start time for the time–of–flight measurements with $\sigma_t \lesssim 30$ ps.

The data presented here were collected with the MRS at 40°, 60°, and 90° and the FS at 4°,8°,12° and 20°. For magnetic fields of the same magnitude but opposite polarities, the spectrometer acceptance is identical for positively and negatively charged particles. Therefore, most systematic errors associated with acceptance and detector efficiency cancel in the particle ratios. In general, the experimental methods employed here are the same as those described in [3].

Figure 1 shows the particle identification capability. Particle yields in the MRS and FS are determined by selecting tracks within a $\pm 2\sigma$ band of the expected β^{-1} vs. momentum behavior for a given particle type. In the FS, additional momentum dependent cuts on the Cherenkov detector signals have been applied. The number of particles measured in various runs is normalized to the number of collision events fulfilling a given centrality cut. The geometrical acceptances of the spectrometers change as a function of the collision vertex and the normalization is done depending on the collision vertex, thus accounting for possible differences in the vertex distributions from run to run. From the normalized number of antiparticles and particles the ratios are calculated.

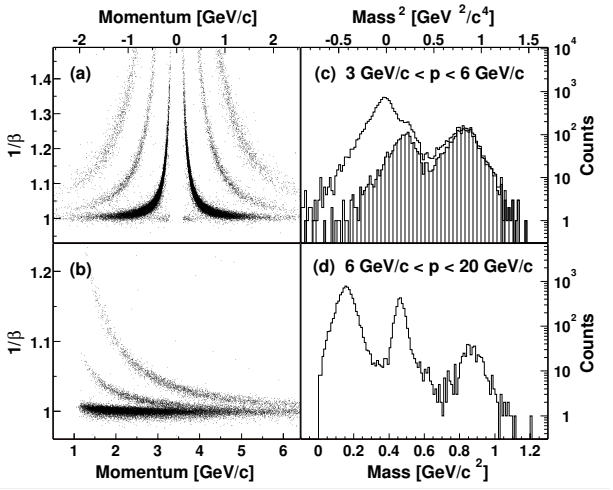

FIG. 1: Particle identification capability in BRAHMS. (a) and (b) Separation between pions, kaons, and protons. The MRS (a) is at 90 deg. and both charges are accepted. The FS (b) is here positioned at 12 degrees. (c) Mass-squared spectrum in the FS from time-of-flight measurements. The shaded histogram includes the vetoing of pions in C1. (d) Mass spectrum in FS using the RICH.

The ratios have been corrected for absorption and production of secondary particles in the material traversed (Be beam tube, various detector elements and air). Losses of antiprotons due to annihilation have been evaluated in GEANT simulations to be about 3% in the MRS and 0.9% in the FS. In the MRS the background contribution to proton yields, arising mainly from the interaction of pions with the beam pipe, is $\approx 10\%$ for the lowest p_T bin at midrapidity falling off to 2 % at $p_T > 0.5$GeV. In the FS this contribution is found to be negligible at the smallest angles and amounts to less than 1% at 30 degrees. For kaons decay losses cancel out, and differences in reaction cross sections for K^- and K^+ amount to less than 1%.

Figure 2 shows the dependence of the ratios for pions, kaons and protons (corrected as described above) on transverse momentum p_T (a and c) and collision centrality (b and d) in two selected rapidity intervals, around y=0 and $y \approx 2$ respectively. The measured ratios show no significant dependence on p_T or cen-

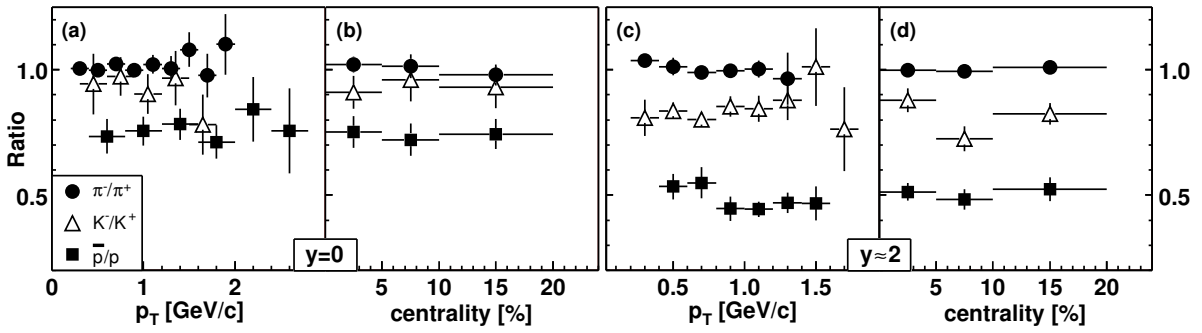

FIG. 2: Dependence of the measured antihadron/hadron ratios on transverse momentum and reaction centrality. The panels to the left are for $y = 0$ and panels to the right for rapidities in the range $y = 2.05$ for protons to $y = 2.55$ for pions.The errors are statistical only.

trality in the covered ranges. Therefore we integrate our yields over centrality in the 0-20% range and over transverse momentum before calculating the ratios.

The ratios shown in Fig. 2 have not been corrected for protons and antiprotons that originate from weak decays of hyperons (Λ, Σ, *etc.*). Corrections for feed down depend on the relative production of hyperons and primary baryons and their antiparticles, and on the respective spectrum slopes. The STAR experiment has recently measured $\Lambda/p \approx 0.5$ and $\bar{\Lambda}/\Lambda = 0.74 \pm 0.04$ at y=0 for $\sqrt{s_{NN}} = 130$ GeV collisions [13]. We have studied the magnitude of the corrections using various model assumptions as input to realistic GEANT simulations of the BRAHMS setup. Assuming primary Hyperon/Baryon ratios similar to those measured by STAR we find that the corrections to the quoted ratios in our acceptance are less than 5%.

Figure 3 shows the π^-/π^+, K^-/K^+ and $\bar{p}/p$ ratios as a function of rapidity. Statistical errors are shown as vertical error bars, while systematic plus statistical errors are indicated by the caps. Systematic uncertainties are estimated as 4% primarily from the normalizations between opposite polarity settings. While the π^-/π^+ ratio is consistent with unity over the considered rapidity range, the K^-/K^+ ratio shows a decrease from 0.95 ± 0.05, at $y = 0$, to 0.67 ± 0.06, at $y = 3.05$. Likewise the $\bar{p}/p$ ratio decreases from 0.75 ± 0.04, at $y = 0$, to 0.23 ± 0.03, at $y = 3.1$. The $\bar{p}/p$ ratio at y=0 exceeds the ratio measured in Au+Au collisions at 130 GeV [3–5] by about 17%. We also note that the $\bar{p}/p$ and K^-/K^+ ratios are essentially constant in the rapidity interval y=0-1. This is consistent with the onset of the boost invariant plateau around midrapidity.

The measured set of particle ratios at midrapidity also lends itself to an analysis in terms of a model based on the assumption of a system in chemical and thermal equilibrium such as has already been advocated for SPS energies. Recently, particle ratios measured at $\sqrt{s_{NN}} = 130$ GeV in the midrapidity region have been analyzed in a Grand Canonical Ensemble (GCE) with baryon number, strangeness and

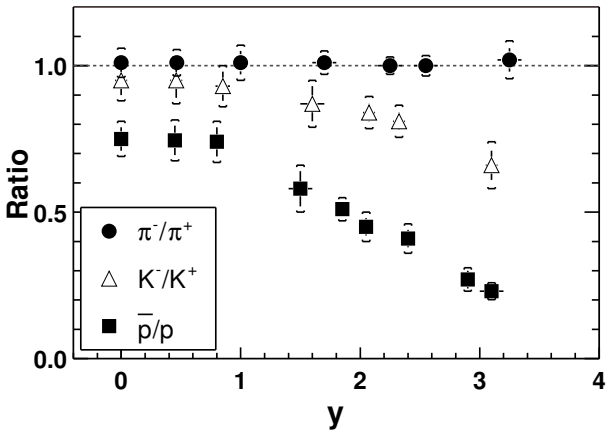

FIG. 3: Antiparticle-to-particle ratios as a function of rapidity. The vertical lines show the statistical errors while the caps indicate the combined statistical and systematic errors.

charge conservation [14]. The relevant parameters of the model are the temperature T and the baryon (or light quark) chemical potential $\mu_B = 3\mu_q$. Values of $T = 174 \pm 7$ MeV and $\mu_B = 46 \pm 5$ MeV were found. In Ref. [14] a parametrization as a function of energy is proposed leading to a prediction for $\sqrt{s_{NN}} = 200$ GeV of $T = 177 \pm 7$ MeV, $\mu_B = 29 \pm 8$ MeV and thus $\bar{p}/p = 0.752$, $K^-/K^+ = 0.932$, and $\pi^-/\pi^+ = 1.004$. We note the excellent numerical agreement between these calculations and the present measurements. Within this approach, the near constancy of the temperature for chemical freeze-out found at SPS, at lower RHIC energies, and at the present energy can be associated with a fixed deconfinement transition temperature and the establishment of chemical equilibrium during hadronization. The small value of the chemical potential indicates a small net baryon density at midrapidity.

Surprisingly, a comparison of the K^-/K^+ and $\bar{p}/p$ ratios over a large range in rapidity and collision energy shows a remarkable correlation as shown in Fig. 4. Ratios are measured at slightly different rapidities. Therefore the K^-/K^+ ratios in Fig. 4 are

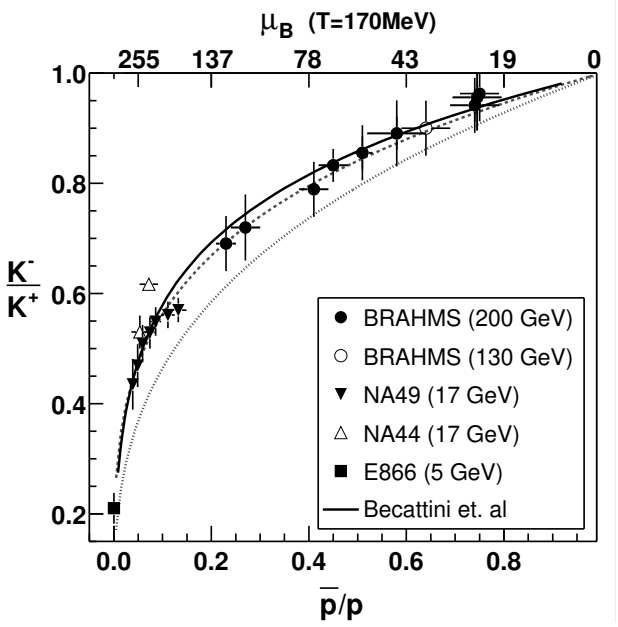

FIG. 4: Correlation between strange meson and baryon antiparticle-to-particle ratios. The NA44 and NA49 data are from Refs. [17] and [16], respectively. The E866 data are from Ref. [15]. The dashed line shows the relation $K^-/K^+ = (\bar{p}/p)^{1/4}$ and the dotted line shows $K^-/K^+ = (\bar{p}/p)^{1/3}$. The full line shows the thermal prediction of Becattini et al.[18].

interpolated to the y value of the $\bar{p}/p$ measurements. Also shown are similar ratios determined at AGS [15] and SPS energies [16, 17]. The figure evidences a smooth relationship between the ratios from AGS and SPS to RHIC, that can be expressed by a power law $K^-/K^+ = (\bar{p}/p)^{1/4}$. Since the compared ratios are not at the same rapidity a thermal interpretation is not strictly justified. Nonetheless, we note that for a vanishing strange-quark chemical potential this exponent is expected to have a value of 1/3. The present result suggests $\mu_s = 1/4 \times \mu_q$. Good agreement is also found by comparing the present data with the thermal model of Becattini et al. [18], which is based on SPS results integrated over the full phase space,and assuming $T = 170$MeV. Within the framework of the statistical model, and assuming that the particle sources corresponding to the different rapidity regions sampled in our experiments are all in local chemical equilibrium subject to strangeness conservation, Fig. 4 therefore suggests that the baryon chemical potential decreases from $\mu_B \approx 130$ MeV, at $y \approx 3$, to $\mu_B \approx 25$ MeV, at y=0.

In summary, the BRAHMS experiment has measured the ratios of charged hadrons at the RHIC top energy and observed the highest such ratios yet in nuclear collisions. We find an increase in the ratio of antiprotons to protons and charged singly-strange mesons, consistent with a significant increase in reaction transparency compared to lower energies. The ratios are, within errors, constant in the interval $y = 0 - 1$ as expected for a boost invariant midrapidity plateau dominated by particle production from the color field. The ratios are well reproduced by statistical model calculations in which the baryon chemical potential decreases strongly from forward rapidities, where the baryon content of the original colliding nuclei is still significant, towards midrapidity. The systematics of kaon and proton ratios suggests a empirical universal relationship between light and strange quark chemical potentials.

This work was supported by the division of Nuclear Physics of the Office of Science of the U.S. DOE, the Danish Natural Science Research Council, the Research Council of Norway, the Polish State Com. for Scientific Research and the Romanian Ministry of Research. We are indebted to F. Becattini for supplying us with thermal model calculations.

[1] N. Herrmann *et al.*, Ann. Rev. Nucl. Part. Sci. **49**, 581 (1999).
[2] H. Satz, Rep. Prog. Phys. **63**, 1511 (2000).
[3] I. G. Bearden *et al.*, BRAHMS Collaboration Phys. Rev. Lett. **87**, 112305 (2001).
[4] C. Adler *et al.*, STAR Collaboration, Phys. Rev. Lett. **86**, 4778 (2001).
[5] B. B. Back *et al.*, PHOBOS Collaboration, Phys. Rev. Lett. **87**, 102301 (2001).
[6] W. A. Zajc *et al.*, PHENIX Collaboration, Nucl. Phys. **A698**, 39c (2002).
[7] I. G. Bearden *et al.*, BRAHMS Collaboration, Phys. Lett. **B523**, 227 (2001).
[8] I. G. Bearden *et al.*, BRAHMS Collaboration, Phys. Rev. Lett. **88**, 202301 (2002).
[9] B. B. Back *et al.*, PHOBOS Collaboration, Phys. Rev. Lett. **88**, 022302 (2002).
[10] J.D. Bjorken, Phys. Rev. **D27**, 140 (1983).
[11] B. B. Back *et al.*, PHOBOS Collaboration, Subm. to Phys. Rev. **C** (2002), nucl-ex/0206012.
[12] M. Adamczyk *et al.*, BRAHMS Collaboration, Nuclear Instruments and Methods, to be published.
[13] C. Adler *et al.*, STAR Collaboration, Submitted to Phys. Rev. Lett. (2002), nucl-ex/0203016.
[14] P. Braun-Munzinger *et al.*, Phys. Lett. **B518**, 41 (2000).
[15] L. Ahle *et al.*, E866 Collaboration. Phys. Rev. Lett. **81**, 2650 (1998) and Phys. Rev.**C60**, 044904 (1999).
[16] Y. Afanasiev *et al.*, NA49 Collaboration, nucl-ex/02050002; J. Bächler *et al.*, Nucl. Phys. **A661**, 45 (1999).
[17] I. G. Bearden *et al.*, NA44 Collaboration, J. Phys. G, Nucl. Part **23**, 1865 (1997).
[18] F. Becattini *et al.*, Phys. Rev. C**64**, 024901 (2001)and

private communication.